Available online at www.sciencedirect.com
ScienceDirect
Procedia Engineering 6 (2010) 44–53
Procedia Engineering
www.elsevier.com/locate/procedia

IUTAM Symposium on Computational Aero-Acoustics
for Aircraft Noise Prediction

LES-Based Evaluation of a Microjet Noise Reduction Concept in Static and Flight Conditions

M. L. Shur[a*], P. R. Spalart[b], M. Kh. Strelets[a]

[a]*New Technologies and Services, 14, Dobrolyubov Ave., St.-Petersburg 197198, Russia*
[b]*Boeing Commercial Airplanes, PO Box 3707, Seattle WA 98124, USA*

Abstract

The Large-Eddy Simulation (LES) numerical system established since 2002 for jet-noise computation is first evaluated in terms of recent gains in accuracy with increased computer resources, and is then used to explore the relatively new "microjet" noise-reduction concept (injection of high-pressure microjets in the vicinity of the main jet nozzle exit), which currently attracts significant attention in the aeroacoustic community. The simulations are found to capture the essential features of the flow/turbulence and the far-field noise alteration by the microjets observed in experiments, and to reveal the subtle flow features responsible for the effect of injection on noise. They also confirm the experimental observation that in static conditions microjets provide a noise reduction comparable with that from chevrons in the low-frequency range, and probably have a less pronounced high-frequency penalty. This positive evaluation of the microjets concept is, however, mitigated by results of simulations in flight conditions, which were never studied experimentally. The latter results, which are awaiting an experimental verification, make a practical use of the concept in its current form rather unlikely.

Keywords: Jet noise prediction; Large Eddy Simulation; Noise-reduction concepts; Microjets

1. Introduction

Over the last decade, LES of turbulence coupled with integral acoustic methods, Ffowcs Williams and Hawkings or Kirchhoff, has made significant progress and proved to be capable of predicting the far-field noise of turbulent jets in the full Mach number and temperature range of interest in commercial aviation to a very useful degree (see, e.g., [1-4]). This justifies the use of such numerical systems to evaluate the performance of jet-noise-reduction devices, which, in fact, is the most important application area for non-empirical methods of jet-noise prediction. Of course, LES alone still cannot resolve all the related issues, first of all, because of the insufficient frequency range and the inability to capture the excessively complex geometry of full industrial cases with pylons, heat shield, vents, etc., with high-order structured CFD codes. These have proven to be most successful in jets aeroacoustics. However,

* Corresponding author. *E-mail address*: mshur@cfd.spbstu.ru

1877-7058
doi:10.1016/j.proeng.2010.09.006

unlike flow measurements, LES provides the entire flow and sound fields thus greatly supporting the design efforts. It also sets no limits to the ambient flow velocity, in contrast with most experimental facilities. An example of numerical system for jet noise prediction supporting the high potential of the LES-based approaches is given in [5-7]. This system established since 2002, has now reached a good level of confidence over a wide range of geometries and flow conditions. Owing to improvements made both to the turbulence simulation and the far-field extrapolation [6, 7], geometries now include dual nozzles, with stagger and with an external core plug; noise-reduction devices such as chevrons and bevels are also routinely treated. This is made possible by a two-stage simulation procedure which includes a coupled nozzle/jet plume RANS computation, in the first stage, and Implicit LES (i.e., without activation of the SGS model) of the jet plume alone, in the second stage. The approach has proven to reproduce the effect of the internal nozzle geometry and maintain realistic boundary layers without the extreme cost of a coupled nozzle-plume LES [8]. Combined with low-dissipative high-order numerics, this ensures a rapid transition to turbulence in the jets shear layer, which is of crucial importance for an accurate noise prediction.

The paper presents a new application of the system [5-7] to the evaluation of noise-reduction devices, namely, of the injection of microjets into the main jet, an idea currently attracting significant attention in both experimental and CFD jet-noise communities as an alternative or a complement to chevron-nozzles. This is preceded by a discussion of recent results of simulations of the simple subsonic M=0.9 jet carried out on much finer grids than those used in our earlier studies [5, 9]. These give an idea of the accuracy increase possible with increasing computer power.

2. Grid-sensitivity study of LES-based noise prediction for M=0.9 round jet

A classic M=0.9 unheated jet is considered, which was analyzed in numerous LES-based jet noise studies including those of the authors [5, 9]. The jet is that from a conical nozzle studied experimentally in [10]. The Reynolds number based on the exit diameter $D = 2.45"$ is equal to $1.1 \cdot 10^6$, and according to a RANS computation inside the nozzle, the nozzle-exit boundary layer thickness and the momentum thickness are $8 \cdot 10^{-3} D$ and $5 \cdot 10^{-4} D$, respectively. In the present work, two new simulations of this jet are carried out on much finer grids than those used in [5, 9]. Table 1 summarizes the major characteristics of both "old" and "new" grids (all dimensions are normalized with D).

Table 1

	Grid 1 [5]	Grid 2 [9]	Grid 3 (present work)	Grid 4 (present work)
Outer block size $N_x \times N_r \times N_\phi$	308×81×64	515×101×80	515×101×160	601×158×240
Total cells count	1.6 M	4.2 M	8.4 M	23 M
Δx at nozzle exit	0.011	0.008	0.008	0.005
Average Δx for 0<x<4	0.033	0.022	0.022	0.016
Average Δx for 4<x<10	0.11	0.055	0.055	0.042
Min Δr in shear layer	0.003	0.0025	0.0025	0.0018
$r\Delta\phi$ in shear layer	0.05	0.04	0.02	0.013

All four grids have the same topology with two overlapping blocks [5], the inner one Cartesian, and the outer one cylindrical. The computational domain extents from 10D upstream to 70D downstream of the nozzle exit. In the radial direction the outer radius of the domain varies from 15D in the vicinity of the nozzle to 30D at the end of the domain. For the far-field noise extraction, a set of nested closed funnel-shaped control FWH surfaces is used, with the narrowest surface placed in immediate vicinity of the turbulent area. Based on the value of Δr at the FWH surface and assuming that 8 cells per wave length are sufficient for a decent representation of sound propagation from source region up-to the control surfaces, the estimates of the highest Strouhal number resolved by the grids are around 2.5 for Grid 1, 7 for Grids 2 and 3, and 12 for Grid 4. Note that Grid 3 differs from Grid 2 only by the doubled number of nodes in the azimuthal direction, whereas in Grid 4 the steps in all the three spatial directions in the "sensitive" flow area are reduced by a factor of about 1.5 compared to Grid 3.

Results of the simulations are presented in Figs. 1-4. In particular, Fig. 1 gives an idea of the turbulent structure of the jet from the simulation on the finest of the considered grids (Grid 4). In line with our previous results obtained on coarser grids, it shows that without any resolved inflow turbulence, a rapid spontaneous transition does occur and

no regular (Kelvin-Helmholtz like) structures are formed in the initial part of the jet shear layer. This is visibly displayed also in Fig. 2, where the distributions are presented of the radial velocity in the mixing layer (with the x and ϕ axes adjusted to give an ratio of 1 between x and $r\phi$), obtained in the simulations on all four grids. The figure demonstrates the rapid three-dimensionalization of the layer, quite natural at the considered high Reynolds number and with a thin boundary layer at the nozzle exit. Note also, that as could be expected, the transition to turbulence is somewhat grid-dependent (it starts earlier with a finer grid).

Figure 3 demonstrates the effect of grid on major mean and statistical aerodynamic characteristics of the jet. It shows that, although grid-independence is not reached uniformly, a trend to convergence is observed, especially considering that the difference between the Grids 3 and 4 is 1.5 times larger than that between the Grids 2 and 3. In terms of agreement of the predictions with the data, overall it improves, but the finest grid results in some overestimation of the length of the potential core compared to experiments. Also, although uniformly reliable experimental data on the Reynolds stresses in the early part of the mixing layer ($x/D<2$) are not available (PIV measurements are known to significantly underestimate the stresses because of insufficient spatial resolution), all the simulations seem to reveal an overshoot of resolved stresses in this region, and grid refinement leads mostly to narrowing of the overshoot extension. Finally, on Grids 3 and 4, the peak values of the stresses in the shear layer are showing signs of a self-similar state with flat behavior up to $x/D\approx 10$.

Moving on to the results of the far-field noise computations presented in Fig.4, it should be noted, first of all, that a trend to grid-convergence in the noise predictions is more definitely pronounced, and that grid refinement results in a distinct improvement of agreement with measurements not only in the high-frequency range, as expected, but also with respect to the spectral maximums at a Strouhal number, *St*, near 1.0 for all the observer angles less than 140°. For the highest resolved frequency, on the finest grid (Grid 4) the upper limit of reliable prediction is as high as $St\approx 12$ (for the one-third octave band) compared to $St\approx 2$ on the coarsest grid (Grid 1). This is already not crucially far from the practically meaningful range of $St=15-20$ and is quite close to the value of $St\approx 15$ in the narrow-band spectra reached in the simulation of Uzun and Hussaini [8] of the jet from a chevron nozzle; it was carried out with resolution of LES content in the near-exit part of the nozzle boundary layer, on a grid with 400 million cells. Note that even with such a grid and a very short (10*D*) computational domain, this, ideally rigorous, approach demanded an artificial reduction of the Reynolds number by a factor of 14 versus the experimental value of $1.4\cdot 10^6$, thus, to a considerable extent negating the rigor of the approach. Considering that the reduced Re number did not prevent accurate prediction of the noise spectra in the jet normal direction up to *St*=15 and, also, that similar accuracy is reached in the present study with no LES-content in the incoming boundary layer, this actually suggests that the latter is not needed for the practically meaningful Re numbers and frequencies.

The largest disagreement with experiment resides at high θ angles, but we note that the rapid change in the spectral shape is not missed by the simulation. The sound level is somewhat insufficient, but the shape change is physically encouraging.

One more important conclusion based on the results presented in Fig. 4 is that even with grids that are quite affordable nowadays in routine computations (Grid 2 from Table 1), the numerical system [5-7] ensures a fairly accurate representation of the jet noise up to *St* around 5. This allows using such modest grids for evaluation of different jet-noise-reduction devices without the risk of missing a "high-frequency penalty" typical of noise-reduction concepts (the "crossover" frequency for all the known concepts is well below *St*=5). Several examples of such applications are presented in [6], [15], where we have considered chevron nozzles, dual nozzles with fan-flow deflecting vanes, and single and dual beveled nozzles.

Below we present one more such example, namely, the evaluation of the microjet noise-reduction concept.

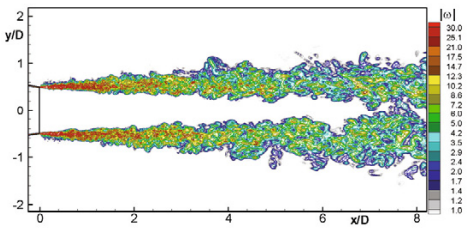

Figure 1: Snapshot of vorticity magnitude in the M=0.9 jet from simulation on Grid 4 from Table 1.

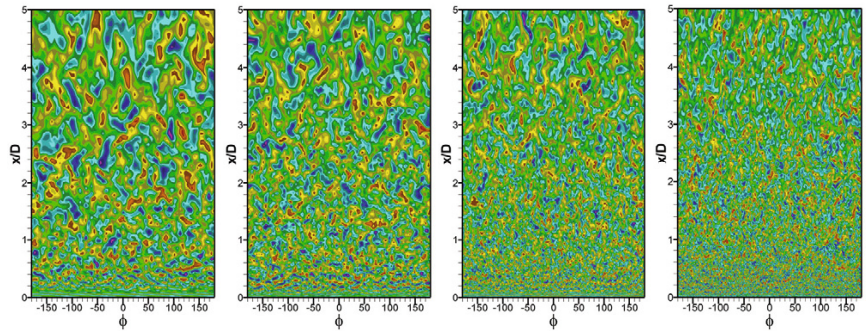

Figure 2: Instantaneous radial velocity u_r on a grid sleeve inside the mixing layer.

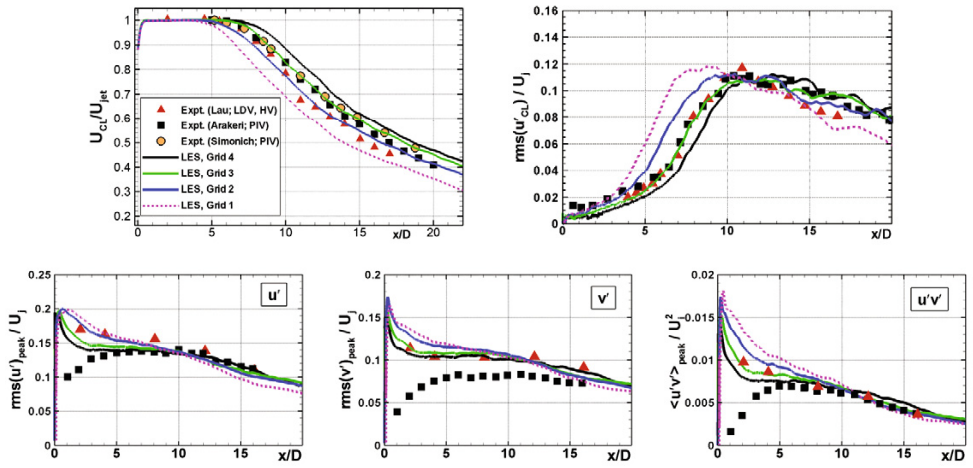

Figure 3: Centerline distributions and peak Reynolds stresses. Data from [11-14].

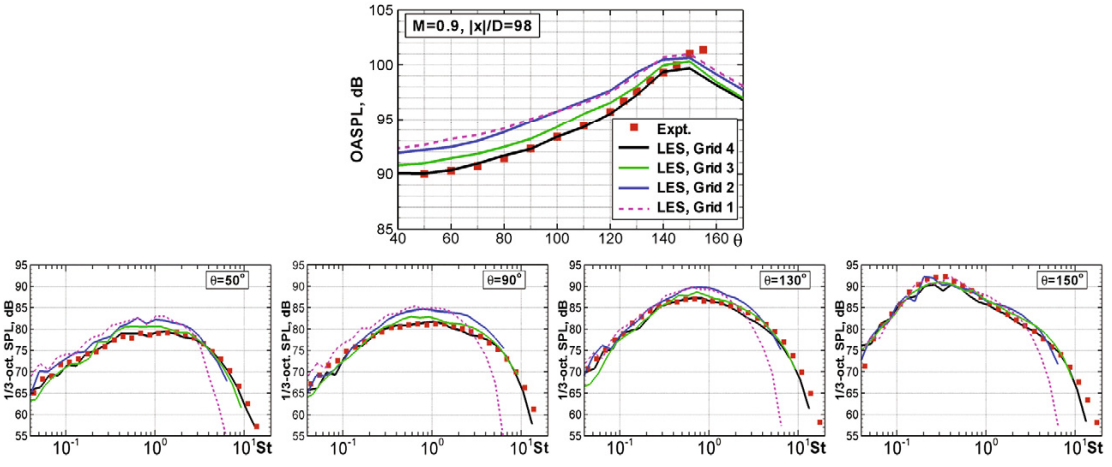

Figure 4: Overall noise directivity and 1/3-octave spectra. Data from [10].

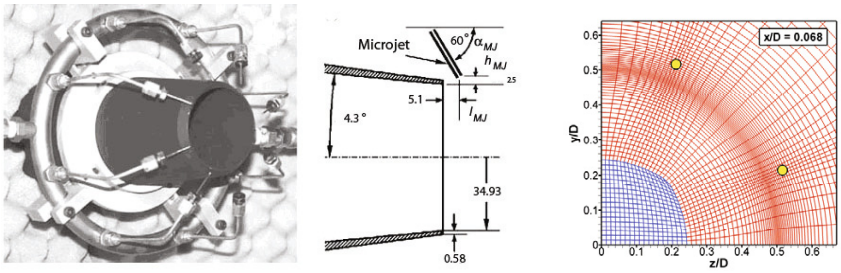

Figure 5: Configuration tested by Alkislar et al. [18] and fragment of LES-grid in YZ-plane in the mircojet injection cross section. Dimensions in the middle frame are in mm. Yellow circles show regions with non-zero source terms in the governing equations emulating microjets.

3. Evaluation of microjet noise-reduction concept

As mentioned, this concept currently attracts attention as a potential alternative to chevron nozzles, with the advantage of activating the control system only when it is needed (e.g., take-off/landing flight stages), thus avoiding the thrust loss in cruise typical of chevrons. A positive effect of microjets (MJ) on the noise was first reported for the supersonic and sonic jets with shocks (see e.g., [16, 17]). For subsonic jets, which are of primary interest for commercial airplanes, experimental investigations of the effect of MJ are mostly restricted to the classic M=0.9 unheated jet [13, 18, 19]. They show that for this jet MJ-injection results in a noise reduction of 0.5-2 dB, depending on the MJ parameters and observer angle and in shifting of the high-frequency noise penalty observed for chevron nozzles to significantly higher frequencies (and, therefore, to lower noise amplitudes). The studies have also indicated a mechanism of the noise reduction caused by MJ. In particular, detailed PIV measurements of the flow and turbulence characteristics carried out in [13, 18] for the configurations with 18 and 8 MJ, respectively, have shown that MJ-injection into the main jet leads to a formation of streamwise vortices which suppress turbulent fluctuations in jet's shear layer.

LES-based studies of MJ available in the literature [20-22] are rather limited. Their major finding is that LES is capable of capturing the effect of MJ on both aerodynamics and jet noise observed in the experiments. In particular, simulations do predict a 1-2 dB medium frequency noise-reduction which is close to the experimental observations. However, even the most complete study with MJ gridding [22] (124 million cells total), does not claim to resolving high frequency (St > 3) noise and, therefore, does not permit to address the high-frequency noise penalty issue. Other than that, neither numerical nor experimental studies consider performance of the device in flight conditions, which is crucial for an assessment of the practical value of the concept. For this reason, the present work focuses on analysis of exactly these insufficiently studied aspects of the microjets, i.e., on their effect in flight conditions and on the evaluation of the attendant high-frequency noise penalty.

The simulations are carried out for the system studied in the experiments [18], which includes 8 equally spaced MJ injected into M=0.9 unheated main jet (see Fig. 5). Similarly to other LES studies [20, 21], the MJ are not gridded but "created" by means of source terms in the governing equations. However, in contrast to these studies, the sources are not confined by only one computational cell but are distributed in space, with appropriate grid clustering in the vicinity of the injection ports (the specific form of the source terms is not presented because of the page limit). This approach ensures a reasonable representation of the microjets' size and local characteristics, although with the present grids, there is no claim to an accurate reproduction of their "internal" turbulence.

In addition to the two simulations (baseline and with MJ) corresponding to the static conditions studied in the experiments [18], two similar simulations are carried out for flight conditions, at external flow Mach number $M_{CF} = 0.2$ as is typical of take-off/landing regimes. The non-dimensional specific (per unit area) MJ mass flow rate parameter $\rho |V|_{MJ} /(\rho_0 c_0)$ was set at 2.5, which corresponds to fully expanded Mach number 1.5 and the total (through all the 8 MJ) mass flow rate around 4 g/s (0.25% of the main jet mass flow rate).

The grid used in all the simulations is similar to Grid 2 for the round jet of the previous section (see Table 1). However, in order to ensure a more accurate representation of the MJ, it is refined in the azimuthal direction in the

vicinity of the MJ as shown in the right frame of Fig. 5. This non-uniformity is smoothly eliminated as the distance from the MJ injection region increases. The *r*-step of the grid is also slightly refined near the radial location of the injection ports. In total, the grid has around 7.6 million cells, with 144 cells in the azimuthal direction.

Moving on to a discussion of results of the simulations presented in Figs. 6-14, we first consider the effect of the microjets on the aerodynamics and turbulent structure of the main jet in static and flight conditions. These results reveal two major trends which help to explain the effect of MJ on noise.

Figure 6, where an isosurface is plotted of the velocity magnitude $|V|=0.5U_{jet}$, visibly displays an intensification of fine-grained turbulence in the immediate vicinity of the MJ injection into the main jet stream and further downstream. This effect is clearly pronounced both in static and flight conditions as demonstrated by Fig. 7, which shows snapshots of the magnitude of vorticity in the meridian jet section passing through the center of a microjet for all the four considered jets. Note that exactly this behavior is probably the reason of the high-frequency noise penalty caused by MJ (see below).

In contrast to this, the large-scale turbulence activity in the shear layer of the main jet becomes weaker with MJ, and the alteration of the large-scale turbulent structures caused by MJ injection is crucially different for the jets in still air and in flight. These trends are illustrated by Fig. 8. It shows that in static conditions, the large-scale turbulent fluctuations in the shear layer associated with global jet's instability are tangibly suppressed in the controlled case. However in flight conditions this stabilizing effect appears to be almost negligible compared to a much stronger stabilization caused by the flight itself. This is supported quantitatively by Fig. 9, which compares the fields of turbulent kinetic energy (TKE), a quantity known to be dominated by large-scale disturbances. Note that a decrease of TKE in the shear layer of the controlled jet in still air is quite consistent with experimental observations [13, 18].

Figure 10 shows the predicted alteration of the centerline distributions of the mean velocity and TKE caused by the MJ. The figure suggests that in line with the experiments for the static jets and consistently with the trends we just described, the injection results in quite a noticeable (around one diameter) elongation of the jet potential core and decrease of the maximum centerline TKE, whereas in flight conditions, the centerline distributions are virtually insensitive to the MJ injection.

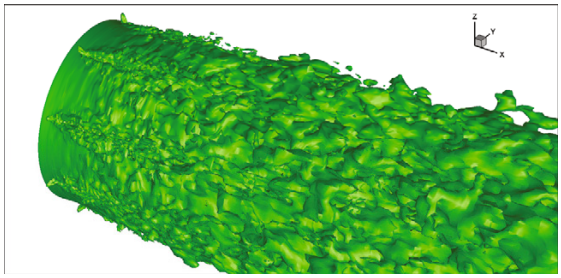

Figure 6: Isosurface $|V|=0.5U_{jet}$ from LES of controlled jet in static conditions.

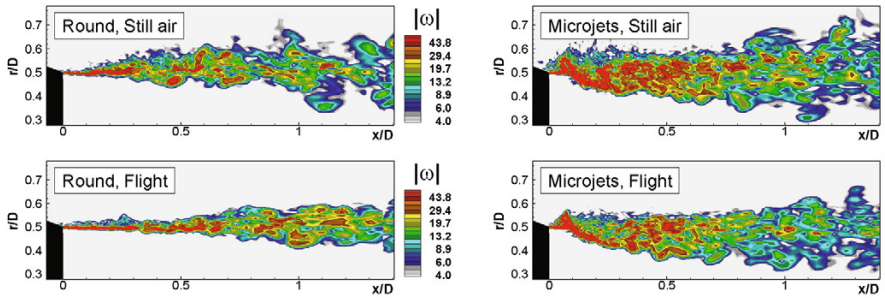

Figure 7: Instantaneous fields of vorticity magnitude in a meridian section passing through microjet center.

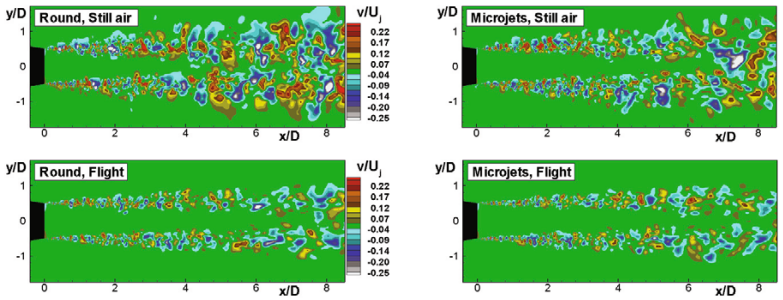

Figure 8: Instantaneous fields of radial velocity in meridian plane between microjets.

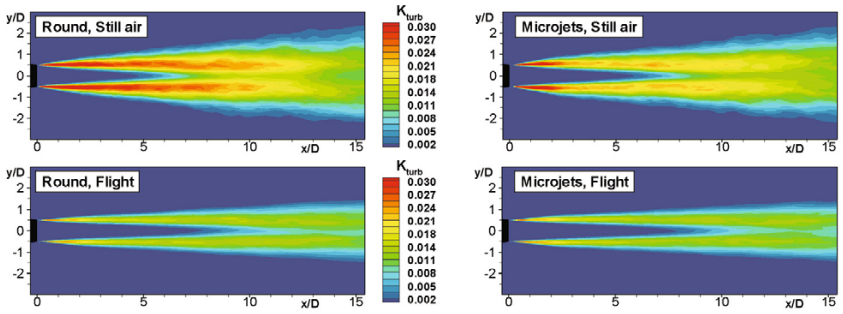

Figure 9: TKE fields in meridian plane between microjets.

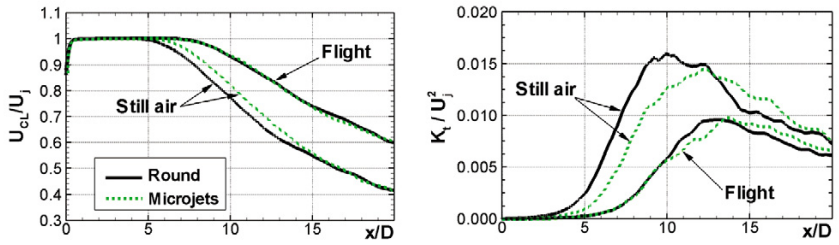

Figure 10: Centerline distributions of mean velocity and TKE.

Let us now discuss the results of computations of major noise characteristics with and without MJ in static and flight conditions, presented in Figs.11-13. In general, all the trends revealed by these figures are consistent with the alteration of the jets aerodynamics and turbulent characteristics analyzed above.

Figure 11 provides a visual qualitative evidence of the positive effect of MJ in static conditions and virtually no effect in flight.

Figures 12, 13 summarize the quantitative information on the effect of MJ on the far-field noise.

Two first columns of Fig.12 compare the MJ effect on the narrow-band noise spectra obtained in the experiment (Fig. 12 a, b) and in the computations (Fig. 12 c, d) for static conditions. The numerical results differ from the experiment, by about the same margin as in figure 4. One can see that the simulations reproduce the MJ effect fairly accurately. Particularly, exactly as in the experiment, with the MJ, the peaks of the computed spectra at low frequencies (St=0.2-0.4) are 1-2 dB lower than for the baseline jet. Also, both in the simulations and experiment, the frequency range of the noise benefit caused by the MJ is rather wide for all the observer angles (only two are shown)

and at large frequencies some noise penalty is observed. Moreover, the predicted crossover frequency, in agreement with the measured one, is around St=3. Note that the noise amplitude at this frequency is already strongly reduced relative to peak levels, and so the high-frequency penalty of the MJ has almost no effect on the integral noise (in practice, the different weightings used in noise certification may alter this tendency). Recall that for chevron nozzles the crossover frequency of the narrow-band spectra can be significantly lower (St=1-1.5, depending on the observer angle), resulting in an increase of the integral noise at close to jet-normal observer angles. Thus, results of the computations support the experimental finding [18] that in this sense MJ injection in static conditions can be more beneficial than chevrons.

A strong difference of the effect of MJ on the far-field noise in flight and static conditions, which could be expected based on the finding concerning the different effect of MJ on the large-scale turbulent activity of the main jet (see Figs. 8, 9), is evident from a comparison of the middle and right columns of Fig.12. One can see that unlike the static conditions, in flight the low-frequency part of the spectra near the spectral peaks is virtually un-affected by the MJ injection (the difference between the baseline and controlled cases is within ~0.5 dB, i.e., does not exceed the accuracy our simulations can claim). At the same time, the high-frequency noise penalty for the controlled jet is of the same order as that for the jet in still air, and the crossover frequencies in flight and in still air are also virtually the same ($St \approx 3$).

As for the OASPL directivity of the noise (see Fig.13), considering that input of the frequencies higher than the crossover one into the integral noise is negligible, it simply reflects the trends discussed above concerning the low-frequency part of the SPL spectra.

Finally, Fig.14 provides some insight into subtle details of the mechanism of the MJ effect on the main jet turbulence and therefore on the noise. In accordance with the experiment [18], the injection of a microjet results in formation of a counter-rotating streamwise vortex pair closer to the high-speed side of the shear layer, which first moves in the radial direction towards the jet axis and then starts moving in the opposite direction (outward in the shear layer). The authors of [18] consider these streamwise vortex pairs as a main reason for the changes in the main jet turbulence suppression discussed above. An analysis of the LES fields suggests a similar, but not identical scenario of the evolution of the mean streamwise vorticity. As seen in Fig. 14a, LES predicts the formation of two rather than one counter-rotating vortex pairs. The inner pair originates from a microjet penetrating inside the main jet and is located close to the high-speed edge of the shear layer. It is rather intensive but dissipates very rapidly. The outer pair forms somewhat farther downstream near the jet half-velocity line. Initially it is much less intensive than the inner pair, but it decays much more slowly. As a result, at $x \approx 0.8D$ the intensities of the two pairs get close to each other. Further downstream, only the outer pair survives and so probably exactly this pair causes the suppression of turbulence in the shear layer. This interpretation is supported by Fig.14b, where we present the downstream evolution of the radial coordinates of the centers of the streamwise vortices from the computations and experiment. The figure suggests that the "2-vortex-pair" scenario, in general, does not contradict the experimental observations and, moreover, permits to explain the non-monotonic evolution of the radial location of the vorticity maximum and the abrupt change of the rate of vorticity decay (not shown) observed in the experiment.

4. Conclusions

LES-based evaluation is carried out of the efficiency of microjet injection for jet-noise suppression in both static and flight conditions. The simulations are performed on a moderately fine grid of about 7.5 million cells, which nonetheless provides resolution sufficient to address the issue of possible high-frequency noise increase caused by the microjets. This capability of the used numerical system is demonstrated by a preceding grid-sensitivity study conducted for a simple round jet, of which the results demonstrate a clear trend to grid convergence in LES-based noise prediction and are of significant interest by themselves.

A major outcome of the microjet simulations is that this noise-reduction concept, considered competitive with chevrons nozzles in static conditions turns out to be virtually "passive" in flight conditions which were never studied experimentally. Specifically, according to CFD, at a typical take-off value of the flight Mach number, the microjet injection does not cause any noticeable reduction of the peak low-frequency noise and still results in the same level of high-frequency noise increase as in static conditions. This finding, which makes a practical use of the concept in its current form rather questionable, is awaiting an experimental verification. Design changes may be tested in the future.

Acknowledgements

This work was funded by Boeing Commercial Airplanes. The authors are grateful to Dr. M. Alkislar for providing experimental data and fruitful discussions.

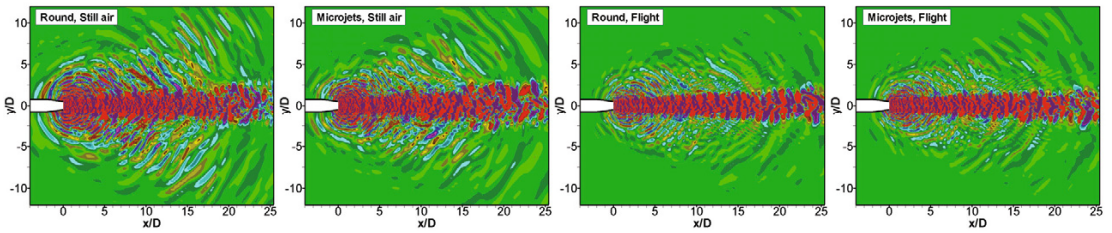

Figure 11: Instantaneous fields of pressure time-derivative in the acoustic range.

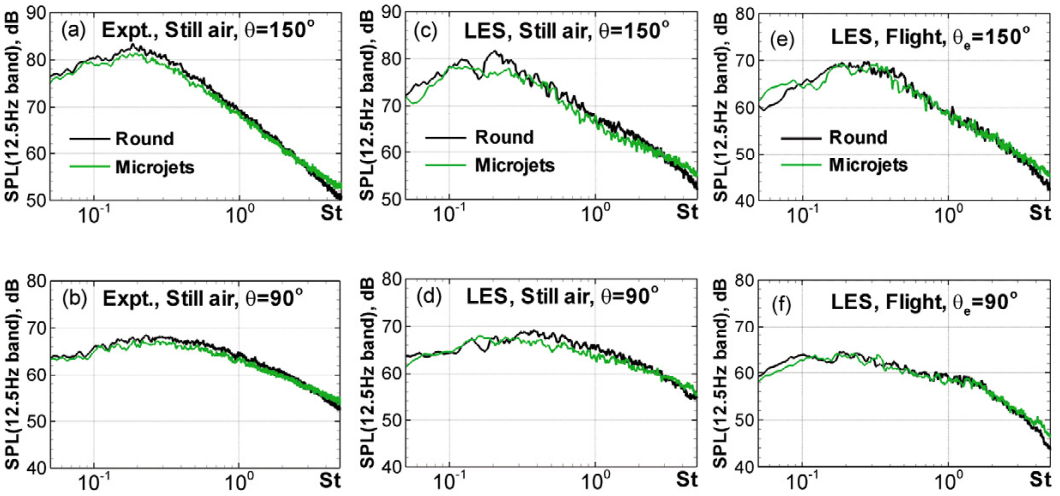

Figure 12: Far-field narrow-band noise spectra. Data (left column) from [18].

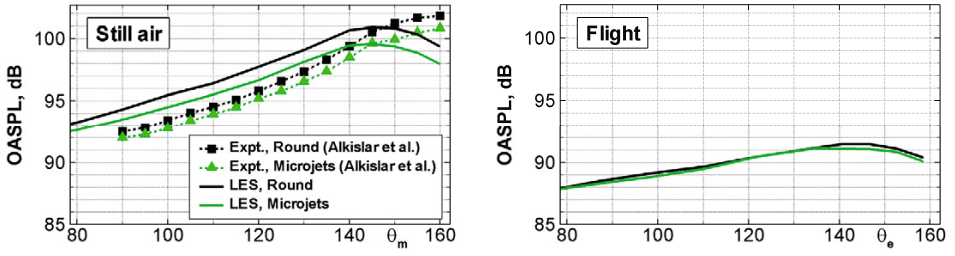

Figure 13: Far-field noise directivity. Data from [18].

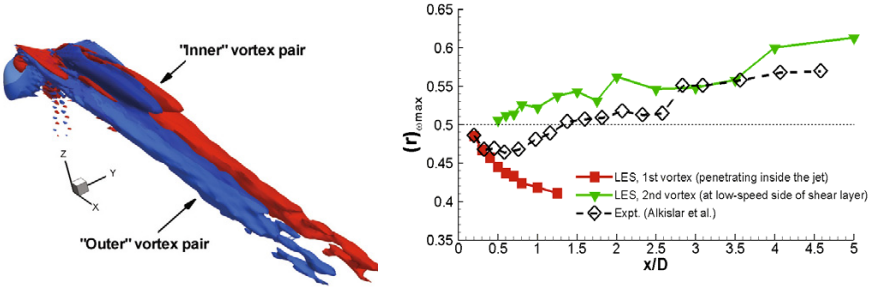

Figure 14: Isosurfaces of mean streamwise vorticity $\omega_x = \pm 0.3$ and radial location of centers of streamwise vortices from LES and experiment.

References

[1] Shur, M.L., Spalart, P.,R., Strelets, M.Kh., Garbaruk, A.V. 2006. "Further Steps in LES-Based Noise Prediction for Complex Jets," AIAA-2006-0485.

[2] Eschricht, D., Greschner, B., Thiele, F., Jacob, M.C. 2009. "Numerical Simulation of Jet Mixing Noise Associated with Engine Exhausts." *Notes on Numerical Fluid Mechanics and Multidisciplinary Design*. **104**, 121-146.

[3] Xia, H., Tucker, P.G., Eastwood, S. 2009. "Large-eddy simulations of chevron jet flows with noise predictions." *Int. J. Heat and Fluid Flow*. **30**(6), 1067-1079.

[4] Mendez, S., Shoeybi, M., Sharma, A., Ham, F.E., Lele, S.K., Moin, P. 2010. "Large-Eddy Simulations of Perfectly-Expanded Supersonic Jets: Quality Assessment and Validation." AIAA-2010-271.

[5] Shur, M.L., Spalart, P.R. & Strelets, M.Kh. 2005. "Noise Prediction for Increasingly Complex Jets. Part I: Methods and Tests. Part II: Applications." *Int. J. Aeroacoustics.* **4**(3+4), 213-266.

[6] Shur, M.L., Spalart, P.,R., Strelets, M.Kh., Garbaruk, A.V. 2007. "Analysis of Jet-Noise-Reduction Concepts by Large-Eddy Simulation," *Int. J. Aeroacoustics.* **6**(3), 243-285.

[7] Spalart, P.R., Shur, M.L. 2009. "Variants of the Ffowcs Williams-Hawkings Equation and Their Coupling with Simulations of Hot Jets." *Int. J. Aeroacoustics.* **8**(5), 477-492.

[8] Uzun, A., Hussaini, M.Y. 2009. "High-Fidelity Numerical Simulation of a Chevron Nozzle Jet Flow." AIAA-2009-3194.

[9] Spalart, P.R., Shur, M.L., Strelets, M.K. 2009. "Added Sound Sources in Jets; Theory and Simulation." *Int. J. Aeroacoustics.* **8**(6), 511-534.

[10] Viswanathan, K. 2004. "Aeroacoustics of Hot Jets." *J. Fluid Mech.* **516**, 39–82.

[11] Lau, J.C. 1981. "Effect of Exit Mach Number and Temperature on Mean-Flow and Turbulence Characteristics in Round Jets." *J. Fluid Mech.* **105**, 193-218.

[12] Lau, J.C., Morris, P.J., Fisher, M. J. 1979. "Measurements in Subsonic and Supersonic Free Jets Using a Laser Velocimeter." *J. Fluid Mech.* **93**, 1–27.

[13] Arakeri, V.H., Krothapalli, A., Siddavaram, V., Alkislar, M.B., Lourenco, L.M. 2003. "On the Use of Microjets to Suppress Turbulence in a Mach 0.9 Axisymmetric Jet." *J. Fluid Mech.* **490**, 75-98.

[14] Simonich, J.C., Narayanan, S., Barber, T.J., Nishimura, M. 2001. "Aeroacoustic Characterization, Noise Reduction.and Dimensional Scaling Effects of High Subsonic Jets." AIAA J. **39**(11), 2062-2069.

[15] Viswanathan, K., Shur, M.L., Spalart, P.,R., Strelets, M.Kh. 2008. "Flow and Noise Predictions for Single and Dual-Stream Beveled Nozzles." *AIAA J.* **46**(3), 601-626.

[16] Krothapalli, A., Greska, B., & Arakeri, V. 2002. "High Speed Jet Noise Reduction Using Microjets." AIAA-2002-2450.

[17] Greska, B., Krothapalli, A., Burnside, N., & Horne, W. 2004. "High-Speed Jet Noise Reduction Using Microjets on a Jet Engine," AIAA-2004-2969.

[18] Alkislar, M.B., Krothapalli, A. & Butler, G.W. 2007. "The Effect of Streamwise Vortices on the Aeroacoustics of a Mach 0.9 jet," *J. Fluid Mech.* **578**, 139-169.

[19] Castelain, T., Sunyach, M., Juve, D. & Bera, J.-C. 2008. "Jet-Noise Reduction by Impinging Microjets: An Acoustic Investigation Testing Microjet Parameters." *AIAA J.* **46**(5), 1081-1087.

[20] Huet, M., Vuillot, F., Rahier, G. 2008. "Numerical Study of the Influence of Temperature and Micro-Jets on Subsonic Jet Noise." AIAA-2008-3029.

[21] Huet, M., Fayard, D., Rahier, G., Vuillot, F. 2009. "Numerical Investigation of the Micro-Jets Efficiency for Jet Noise Reduction." AIAA-2009-3127.

[22] Lew, P.-T., Najafiyazdi, A., Mongeau, L. 2010. "Unsteady Numerical Simulation of a Round Jet with Impinging Microjets for Noise Suppression." AIAA-2010-18.